

## Supplementary Information for

# Basic metal carbonate supported gold nanoparticles: enhanced performance in aerobic alcohol oxidation

Jie Yang<sup>a,b</sup>, Yejun Guan,<sup>a</sup> Tiny Verhoeven,<sup>a</sup> Rutger van Santen,<sup>a</sup> Can Li<sup>b,\*</sup>  
and Emiel J. M. Hensen<sup>a,\*</sup>

<sup>a</sup> *Schuit Institute of Catalysis, Eindhoven University of Technology, P.O. Box 513, 5600 MB Eindhoven, the Netherlands e.j.m.hensen@tue.nl*

<sup>b</sup> *State Key Laboratory of Catalysis, Dalian Institute of Chemical Physics, Chinese Academy of Sciences, Zhongshan Road 457, Dalian, China. E-mail: canli@dicp.ac.cn*

### Contents

X-ray diffraction of zinc hydroxycarbonate.....	S2
Transmission electron microscopy.....	S3
X-ray photoelectron spectroscopy .....	S4
References.....	S5

### *X-ray diffraction of Zinc hydroxycarbonate*

Figure S1 shows the XRD pattern of  $\text{Zn}_3\text{CO}_3(\text{OH})_4$  (label vendor). The pattern most closely resembles powder diffraction data of hydrozincite ( $\text{Zn}_5(\text{CO}_3)_2(\text{OH})_6$ ; ICDD 72-1100) and other zinc hydroxycarbonates such as  $\text{Zn}_4\text{CO}_3(\text{OH})_6$ . The relatively broad lines are indicative of the microcrystalline character of the support material in line with the electron micrographs.

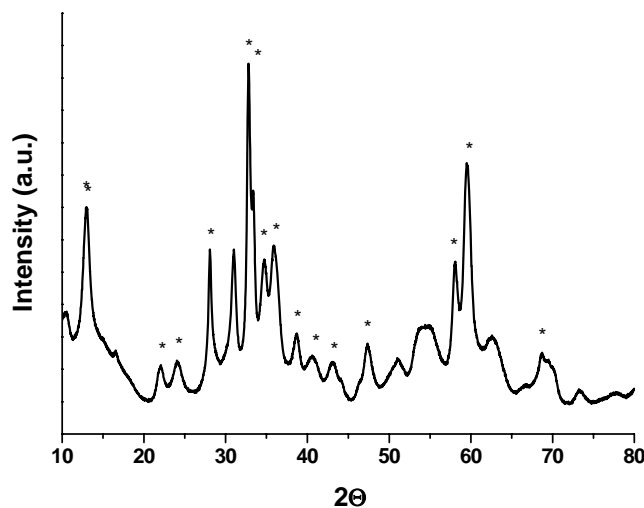


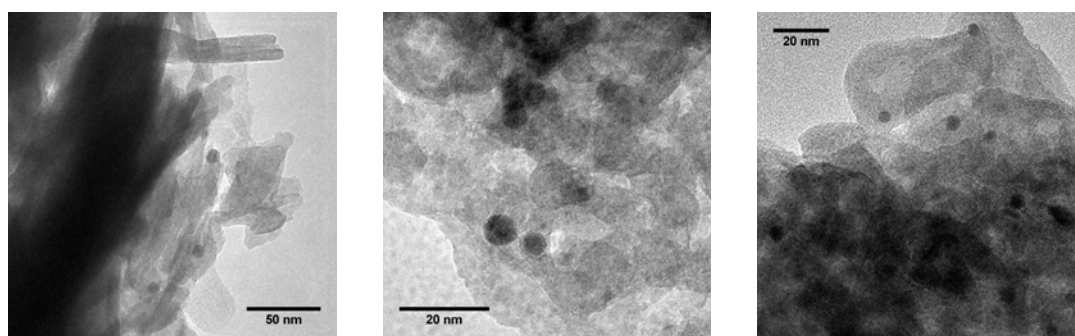
**Figure S1.** XRD pattern of Zn support which identifies the material as hydrozincite.

The XRD patterns of the other supports were also recorded. The pattern of Ce corresponded to those of cerium hydroxycarbonates, that of La matched the powder diffraction data of  $\text{LaCO}_3\text{OH}$  and that of Bi corresponded to data of several bismuth oxycarbonates. The pattern of zirconium carbonate did not show clear reflections.

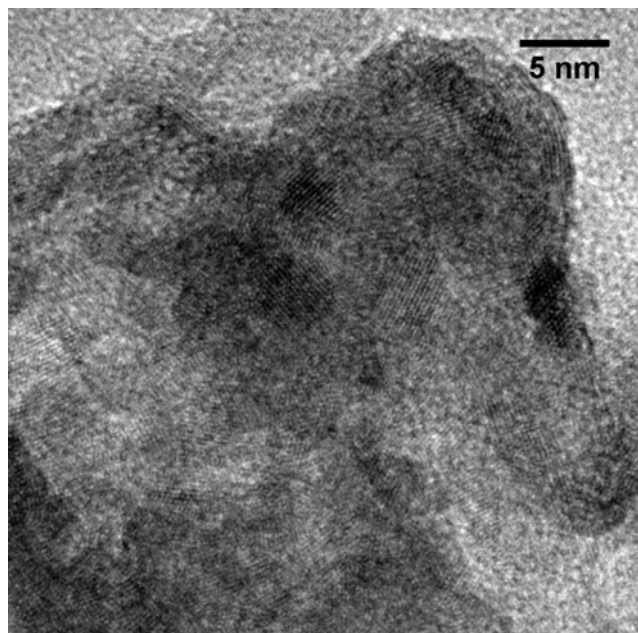
### *Transmission electron microscopy*

Figure S2a shows the electron micrographs of Au/Zn after various treatments. We found that initial reduction by ethanol or during heating in benzylic alcohol led to Au nanoparticles in the range of 4-6 nm (after synthesis 7-9 nm as evidenced by TEM of the sample in water). The microcrystalline character of the hydrozincite support is evident from Figure S2b.

The size distribution of gold nanoparticles in Au/Zn, Au/BiC and Au/Ce is shown in Figure S2c. For these materials at least 50 particles were counted. In Au/La only a few nanoparticles were found and in Au/ZrC none.



**Figure S2a.** Electron micrographs of (left) fresh Au/Zn (brought on the TEM grid in water), (middle) Au/Zn reduced in benzylic alcohol at 373 K and (right) Au/Zn after three consecutive catalytic cycles.



**Figure S2b.** Electron micrographs of the bare zinc hydroxycarbonate support showing its microcrystalline character.

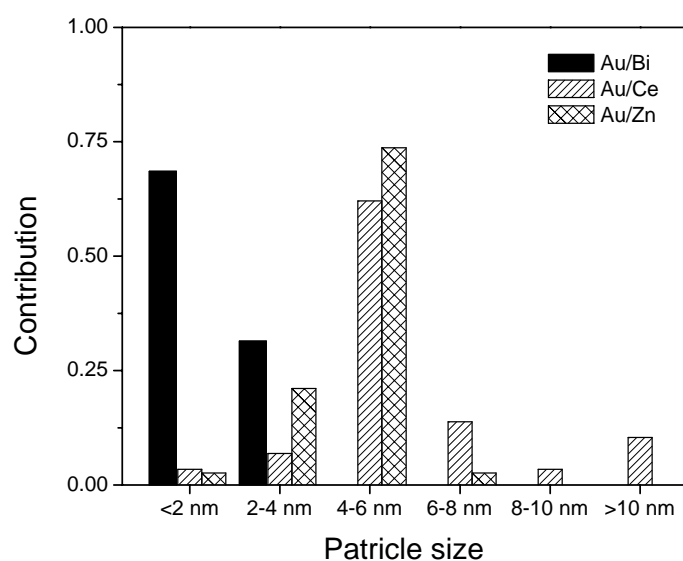


**Figure S2c.** Size distribution of gold nanoparticles for Au/Bi, Au/Ce and Au/Zn.

#### *X-ray photoelectron spectroscopy*

Figure 2 contains the XP spectra of some of the gold-containing catalysts including the fits. The fit results are collected in Table 1. The XP spectrum of Au/Zn was also recorded but fitting of the Au 4*f* region proved impossible because it overlapped with the much more intense Zn 3*p* feature. On the Bi support, the gold nanoparticles are in the metallic form with a Au 4*f*<sub>7/2</sub> at 83.8 eV (referenced to C 1s at 284.6 eV).<sup>1</sup> The XP spectrum could be fitted with a single 4*f* doublet with a slight asymmetry of the peak shape (tailing to higher binding energy). For the Ce support, the XP spectrum included three Au 4*f* features at 83.6 eV, 84.4 eV and 86.6 eV. The value at 83.6 eV is indicative of bulk Au formation. The value at 86.6 eV points to the presence of Au<sup>3+</sup> species as it is intermediate to values found for Au(OH)<sub>3</sub> (87.7 eV) and for Au<sub>2</sub>O<sub>3</sub> (86.4 eV).<sup>2,3</sup> The value at 84.4 eV is considerably higher than that of bulk Au and has been attributed to positively charged Au species, probably Au<sup>+</sup>.<sup>4,5</sup> The presence of this oxidation state has been linked to very small (< 2 nm) Au particles.<sup>6</sup> In Au/Ce the distribution of the various oxidation states Au<sup>0</sup>:Au<sup>+</sup>:Au<sup>3+</sup> is 65:12:23. Fitting the XP spectrum of Au/Zr also necessitated the inclusion of several Au oxidation states. The one at 84.4 eV is again attributed to Au<sup>+</sup> oxidation state and the one at 86.8 eV to Au<sup>3+</sup> states. The contribution of Au<sup>+</sup> is dominant (63%). After reduction of Au/Zr in H<sub>2</sub> at 523 K, a clear shift of the Au 4*f* binding energy is observed. The Au phase is now made up of metallic Au at a 4*f*<sub>7/2</sub> binding energy of 83.5 eV (79%) while the contribution of Au<sup>+</sup> at 86.5 eV has decreased to 21%.

## References

1. J.F. Moulder, W.F. Stickle, P.E. Sobol and K.D. Bomben, *in* Handbook of X-ray Photoelectron Spectroscopy, Perkin–Elmer Corporation, Physical Electronics Division, Eden Prairie, 1992.
2. J.N. Lin and B.Z. Wan, *Appl. Catal. B*, 2002, **1257**, 1.
3. E.D. Park and J.S. Lee, *J. Catal.*, 1999, **186**, 1.
4. L. Fan, N. Ichikuni, S. Shimazu and T. Uematsu, *Appl. Catal. A*, 2003, **246**, 87.
5. R. Si and M. Flytzani-Stephanopoulos, *Angew. Chem. Int. Ed.*, 2008, **47**, 2884.
6. C.N. Rao, V. Vijayakrishnan, H.N. Aiyer, G.U. Kulkarni and C.N. Subbanna, *J. Phys. Chem.*, 1993, **97**, 11157.